

NASA CONTRACTOR REPORT 187594

110 39
61470
P-32

ANALYSIS OF DELAMINATION IN CROSS PLY LAMINATES INITIATING FROM IMPACT INDUCED MATRIX CRACKING

S. A. Salpekar

Analytical Services and Materials, Inc.
Hampton, VA

Contract NAS1-19399

November 1991



National Aeronautics and
Space Administration

LANGLEY RESEARCH CENTER
Hampton, Virginia 23665-5225

(NASA-CR-187594) ANALYSIS OF DELAMINATION
IN CROSS PLY LAMINATES INITIATING FROM
IMPACT INDUCED MATRIX CRACKING (Analytical
Services and Materials) 32 p CSCL 20K

N92-15401

Unclas
63/39 0061470

ABSTRACT

Several two dimensional finite element analyses of ($0_2/90_8/0_2$) glass/epoxy and graphite/epoxy composite laminates were performed to investigate some of the characteristics of damage development due to an impact load. A cross-section through the thickness of the laminate with fixed ends, and carrying a transverse load in the center was analyzed. Inclined matrix cracks such as those produced by low velocity impact were modelled in the 90 degree ply group. The introduction of the matrix cracks caused large interlaminar tension and shear stresses in the vicinity of both crack tips in the 0/90 and 90/0 interfaces. The large interlaminar stresses at the ends of the matrix cracks indicate that matrix cracking may give rise to delamination. The ratio of mode I to total strain energy release rate, G_I/G_{Total} , at the beginning of delamination, calculated at the two (top and bottom) matrix crack tips was 60 percent and 28 percent, respectively, in the glass/epoxy laminate. The corresponding ratio was 97 percent and 77 percent in the graphite/epoxy laminate. Thus, a significant mode I component of strain energy release rate may be present at the delamination initiation due to an impact load. The value of strain energy release rate at either crack tip increased due to an increase in the delamination length at the other crack tip and may give rise to an unstable delamination growth under constant load.

NOMENCLATURE

b, d	delamination lengths from matrix crack tips measured along the x-axis
E_{11}, E_{22}, E_{33}	modulus of elasticity of a unidirectional lamina
G	strain energy release rate
G_{Total}	total strain energy release rate
G_I, G_{II}	Mode I and Mode II components of strain energy release rate, respectively
G_{12}, G_{13}, G_{23}	shear moduli of a unidirectional lamina
h	ply thickness
P	transverse load per unit width
x_b, x_d	distances along lines BA and CD, respectively
x, y, z	Cartesian coordinates
θ	fiber angle in degrees, measured counter-clockwise from x-axis
$\nu_{12}, \nu_{13}, \nu_{23}$	Poisson's ratio of a unidirectional lamina
σ_z	interlaminar normal stress
τ_{xz}	interlaminar shear stress

1. INTRODUCTION

Laminated composites have been shown to be useful materials in many structural applications. These composites must be designed to withstand the service loads. In particular, the low velocity impact on such materials may cause internal damage and will lower the load carrying capacity of the parts. Impact damage development has been investigated extensively in the literature. Some of the recent studies are found in references [1-6]. The low velocity impact has been observed to cause the formation of matrix cracks due to transverse shear stresses, with the matrix cracks inclined at 45 degrees to the direction of the laminate thickness corresponding to the principal tension stress direction [2,6]. These matrix cracks may also be accompanied by delaminations [2,6]. This damage is schematically shown in figures 1(a,b), reproduced from reference 3. Figure 1(a) shows a Quasi-isotropic, graphite/epoxy laminate subjected to low velocity impact (4-16 ft/sec). The damage is in the form of spiral staircase, with delaminations bounded between matrix cracks in successive layers. Three cross-sections of the damaged plate are shown in figure 1(b) in which the matrix cracks appear to be inclined at approximately 45 degrees to the plane of the corresponding lamina. In the absence of matrix cracks, only shearing stresses exist along the ply interfaces which suggests mode II delamination growth. However, the presence of matrix cracks may introduce tensile stresses on these interfaces and cause a significant mode I component. For example, in reference 5, delaminations from the back surface cracking of $[90_4/0/\pm 45]_S$, $[90_4/0_3]_S$, and $[90_3/0/\pm 45]_S$ graphite/epoxy laminates due to impact load was studied. The study concluded that the opening mode (Mode I) component of delamination growth from a matrix

crack may be much larger than the component due to interlaminar shear (Mode II).

The purpose of this paper is to perform stress analyses of a simple laminate configuration to evaluate the effect of simulated low velocity impact damage on the stress state in the laminate. Two dimensional finite element analyses of $[0_2/90_8/0_2]$ glass/epoxy and graphite/epoxy laminates were performed. The laminates were assumed to contain through-thickness, inclined matrix cracks in the 90 degree ply group like those induced by impact. The laminate is subjected to a static central line load. The interlaminar stresses in the 0/90 and 90/0 interfaces were calculated in the vicinity of the matrix cracks. Mode I and II components of strain energy release rate were calculated for delaminations growing from the crack tips.

2. ANALYSIS

2.1 LAMINATE CONFIGURATION AND LOADING:

Graphite/epoxy and glass/epoxy laminates having a $(0_2/90_8/0_2)$ layup, and subjected to a transverse line load in the center (figure 2), were analyzed using the finite element method. The laminate is $550h$ long, where h is the ply thickness, and is fixed on two of its edges as shown in figure 2. The laminate width (y-direction) was assumed large compared to its total thickness (z-direction). A unit ply thickness was assumed in the model. Two matrix cracks, inclined at 45 degrees in the thickness plane, are located in the central 90° group of plies. These matrix cracks are symmetrically located on either side of the line load and extend through the laminate width.

Because the laminate width was large compared with the thickness, and because the load and the matrix cracks extend through the width, the strains were assumed to be zero in the y-direction. Thus, only the x-z plane of the laminate was analyzed using the finite element method. Due to the laminate symmetry about the load line, only the right half of the cross-section as shown in figure 3 was analyzed. The Cartesian coordinate system with its origin at point E is shown in figure 3. The laminate was assumed to be fixed at the right end ($x=275h$) and the symmetry boundary condition was applied at the left end ($x=0$). A unit load was applied at $x=0$ at the top of the laminate. A 45° matrix crack BC was assumed to be present and the crack tip B is located at $x=40h$. Delamination growth was modelled along the 0/90 interfaces from the crack tips (i.e. along BA and CD). The elastic material properties of glass/epoxy and graphite/epoxy used in the analysis are shown in Table 1 and are considered accurate for obtaining qualitative results.

2.2 FINITE ELEMENT MESH:

The finite element discretization of the 2-D model of the laminate used in the analysis is shown in figure 4. A finely graded mesh is used around the inclined crack and around the 0/90, 90/0 interfaces where delamination growth was modelled. A total of 1200 8-node isoparametric parabolic elements having 3825 nodes were used in the model. The delaminations along BA and CD (figure 3) were simulated by releasing coincident multi-point constraints provided in the model.

2.3 INTERLAMINAR STRESSES:

The interlaminar stresses in the 0/90 and 90/0 interfaces near the crack tip were calculated in the uncracked and cracked models subjected to the

transverse load. The locations of high interlaminar stresses indicate the site for delamination onset.

2.4 STRAIN ENERGY RELEASE RATE (G):

The delamination growth was modelled from the two crack tips (B, C) of the matrix crack (fig.3). The delamination from crack tip B in the 0/90 interface was assumed to extend along BA and the delamination from crack tip C extends along CD in the 90/0 interface. This delamination growth was based on experimental observations in similar laminates [6]. The delamination length b along BA was increased with the delamination length d along CD held constant. Similarly the length d along CD was increased for a fixed value of b . The total strain energy release rate (G_{Total}) and its two components G_I & G_{II} were calculated for small increments of delamination growth. The virtual crack closure technique (VCCT) was used to compute the strain energy release rate [7,8].

For delaminations at the interface of two different materials, the values of G_I and G_{II} computed by VCCT do not converge when the finite element mesh is refined [9,10]. However, the values of G_{Total} do converge. The smallest element size ($0.25h$) used here to simulate the delamination growth is considered satisfactory to give qualitative results [10]. The results are presented in the form of normalized strain energy release rate values, ($G E_{11} h / P^2$), where E_{11} is the axial modulus, h is the ply thickness, and P is the load per unit width.

3. RESULTS AND DISCUSSION

3.1 INTERLAMINAR STRESSES:

GLASS/EPOXY LAMINATE

Figure 5 shows the interlaminar normal stress, σ_z , normalized by h/P , along AB. A similar variation was observed near crack tip C along DC. The interlaminar normal stresses, σ_z , in the 0/90 interface along AB (distance x_b in figure 3) and in the 90/0 interface along DC (distance x_d in figure 3) is zero in the uncracked laminate. In contrast, with a matrix crack along BC in the 90 degree group of plies, the tensile interlaminar normal stresses, σ_z , were large in the vicinity of crack tips B and C along AB and DC, respectively. The high gradients of interlaminar tension stress in the 0/90 and 90/0 interfaces indicate crack tip singularities that may initiate delamination at crack tips B and C.

The variation of the stress τ_{xz} along BA with and without matrix crack BC is shown in figure 6. The normalized interlaminar shear stress, $\tau_{xz} h/P$, in the 0/90 and 90/0 interfaces exhibits a high stress gradient in the vicinity of the crack tips B and C due to the presence of the matrix crack BC. In the absence of the matrix crack, the stress τ_{xz} is nearly uniform along the interfaces and has a small value. The variation along DC near crack tip C was found to be similar to that near crack tip B. This stress may also contribute to the delamination onset at points B and C.

3.2 STRAIN ENERGY RELEASE RATE:

3.2.1 GLASS/EPOXY LAMINATE

The delamination growth was first modelled along BA (fig.3) initiating from crack tip B with no delamination at the crack tip C (i.e. $d=0$). The strain energy release rate was calculated at the delamination tip A. The delamination increments were one quarter of a ply thickness. Figure 7 shows the plots of G_I , G_{II} , and G_{Total} at the delamination tip, normalized by $P^2/E_x h$, as a function of the normalized distance b/h . A significant mode I component is present near point B, where the G_I/G_{Total} ratio is 60 percent at $b/h = 0.25$. The G_I component increases with increasing b/h for $b/h \leq 3.5$ while the value of G_{II} decreases with increasing b/h . The magnitude of G_{Total} , which is the sum of the mode I and mode II components, decreases initially, up to $b/h = 1$, and increases due to further delamination growth for $b/h \leq 3.5$. The G_{Total} calculated from the change in global energy due to delamination growth [10] is shown by open circle symbols in figures 7-10. The values are in agreement with G_{Total} using VCCT.

Figure 8 displays the normalized values of G_I , G_{II} , and G_{Total} variation at delamination tip A, when a fixed delamination of 2 ply thickness is assumed along CD instead of no delamination as in the previous figure. The shapes of the curves are similar to those in figure 7. The values of G_I and G_{Total} are elevated significantly by the presence of a delamination along CD. The values of G_{II} are mostly unaffected.

The change in normalized values of G_I , G_{II} , and G_{Total} at delamination tip D as a function of d/h is plotted in figure 9 for the case of no delamination at crack tip B (i.e. $b=0$). In contrast to growth along BA, the ratio G_I/G_{Total} at the beginning of the delamination at crack tip C is 28 percent and decreases with increasing d/h , and the G_{II} component increases with the increase in d/h . The G_{Total} increased by about 25 percent over a four ply delamination distance.

The variation in normalized values of G_I , G_{II} , and G_{Total} at delamination tip D as a function of d/h with a delamination at crack tip B ($b=2h$), is shown in figure 10. The G_I and G_{II} components have almost equal values for $d/h=0.25$. As in figures 7 & 8, G_I and G_{Total} are elevated by the delamination along AB (remote crack tip delamination) and G_{II} is nearly unaffected. The shapes of the curves are similar to those in figure 9 where b was assumed to be zero.

The normalized G_{Total} plots of figures 7-10 are displayed in figure 11 for comparison. As pointed out in figures 7-10, G_{Total} at delamination tip A is larger for all delamination lengths along AB when a delamination is present at the other crack tip (e.g. $d=2h$ versus $d=0$). Similarly, G_{Total} at delamination tip D is higher for all delamination lengths along CD when a delamination is present at the other crack tip (e.g. $b=2h$ versus $b=0$). Also, G_{Total} for tip A increases with delamination growth at tip A and for tip D with growth at tip D. This indicates that once the delamination initiates at crack tip C, the likelihood of delamination onset at B is greater, and vice versa. This increase in G for delamination at one crack tip due to growth at

the other crack tip may lead to unstable delamination growth analogous to the unstable delamination that occurs in tapered laminates subjected to tension loading [11].

Figure 12 shows the plots of G_I as a function of delamination distance, from figures 7-10, displayed together for comparison. The mode I component at delamination tip A is higher than that at tip D for the corresponding cases (e.g. $d=0$ vs $b=0$; $d=2h$ vs $b=2h$). The delamination will initiate at tip B and may cause the G_I at C to increase, similar to that in figure 11.

Figure 13 shows plots for G_{II} , similar to those displayed in figure 12. Unlike G_I and G_{Total} , G_{II} for one delamination tip is relatively unaffected by growth at the other location.

3.2.2 GRAPHITE/EPOXY LAMINATE:

A graphite/epoxy laminate was analyzed for the delamination growth along BA (FIG.3) when the delamination at crack tip C is assumed to be zero ($d=0$). The quantities G_I , G_{II} and G_{Total} were computed. The results of the computation are shown in the left half of figure 14. In a similar manner, the delamination was grown along CD, while the delamination distance b was assumed to be zero. The corresponding G_I , G_{II} and G_{Total} are shown in the right half of figure 14. The G_I/G_{Total} ratio is 97 percent at delamination tip A for $b/h = 0.25$ while the same ratio is 77 percent at delamination tip D for $d/h = 0.25$. Thus a significant mode I component exists at delamination tips A and D.

The variation of the strain energy release rates as a function of delamination distance for the graphite/epoxy material is similar to that of

the glass/epoxy material. However, the G_I and G_{Total} values are larger for graphite/epoxy than for the glass/epoxy material.

4. CONCLUDING REMARKS

In this study, $(0_2/90_8/0_2)$ glass/epoxy and graphite/epoxy laminates containing simulated impact damage were analyzed using a two dimensional finite element analysis. The laminate was assumed to be fixed at its ends, and a transverse line load was applied at the center. Two transverse shear-induced matrix cracks, typical of impact loading, were assumed in the 90 degree ply group. The matrix cracks had a 45 degree inclination in the thickness direction and were assumed to be symmetric with respect to the transverse line load. The strains in the width direction were assumed to be zero and a cross-section through the thickness of the laminate was analyzed. The interlaminar stresses due to matrix cracking and the strain energy release rates for small delaminations (4 ply thicknesses) extending from either end of the matrix crack were evaluated. The results of the analyses are summarized below.

1) The introduction of the matrix crack creates high interlaminar tension and shear stresses at the matrix crack tips. The sharp stress gradients suggest that the matrix crack results in interlaminar stress singularities that cause delaminations between 0/90 and 90/0 interfaces.

2) The mode I to total strain energy release rate ratio, G_I/G_{Total} , was computed for the delamination initiation from either of the crack tips. The values of G_I/G_{Total} at the upper and lower crack tips were 60 percent and 28

percent, respectively, for glass/epoxy material. In the case of graphite/epoxy material, the values of G_I/G_{Total} at the upper and lower crack tips were 97 percent and 77 percent, respectively. These results clearly demonstrate that a significant mode I component is present along with mode II component at the beginning of delamination.

3) The influence on G_I and G_{Total} at one delamination tip due to delamination growth at the other crack tip was determined for the glass epoxy laminates. G_I and G_{Total} at either the upper or lower matrix crack tip increase with increasing length for an assumed delamination at the other matrix crack tip. This indicates that once the delamination initiates, it may grow in an unstable manner at both crack tips.

5. ACKNOWLEDGEMENT

This work was performed under NASA contract NAS1-18599.

6. REFERENCES

- [1] E.F. Dost, L.B. Ilcewicz, and J.H. Gosse, "Sublamine Stability Based Modeling of Impact-Damaged Composite Laminates," Proceedings of the American Society for Composites, Third Technical Conference, Seattle, Washington, September 25-29, 1988.
- [2] J.H. Gosse and P.B.Y. Mori, "Impact Damage Characterization of Graphite/Epoxy Laminates," Proceedings of the American Society for

Composites, Third Technical Conference, Seattle, Washington, September 25-29, 1988.

[3] J.H. Gosse and L.R. Hause, "A Quantitative Nondestructive Evaluation Technique for Assessing the Compression-after-impact Strength of Composite Plates," Proceedings of Progress in Quantitative Nondestructive Evaluation, Volume 7B, 1987.

[4] C.C. Poe, Jr., et. al., "Comparison of Impact Results for Several Polymeric Composites over a Wide Range of Low Impact Velocities," NASA ACT Conference, NASA CP-3104, Part 2, NASA Langley Research Center, Hampton, VA., 1991.

[5] G.B. Murri and E.G. Guynn, "Analysis of Delamination Growth from Matrix Cracks in Laminates Subjected to Bending Loads," Composite Materials: Testing and Design (Eighth Conference), ASTM STP 972, J. D. Whitcomb, Ed., American Society for Testing and Materials, Philadelphia, 1988, pp. 322-339.

[6] F.K. Chang, H.Y. Choi, and H.S. Wang, "Damage of Laminated Composites due to Low-Velocity Impact," Proceedings of the American Institute of Aeronautics and Astronautics, AIAA-90-0915-CP, 1990.

[7] Rybicki, E.F., and Kanninen, M.F., "A Finite Element Calculation of Stress-Intensity Factors by a Modified Crack-Closure Integral," Engineering Fracture Mechanics, Vol. 9, 1977, pp. 931-938.

[8] Raju, I.S., "Calculation of strain-energy-release rates with Higher Order and Singular Finite Elements." Engineering Fracture Mechanics, vol.28, 1987, pp. 251-274.

[9] C.T. Sun and C.J. Jih, "On Strain Energy Release Rates for Interfacial Cracks in Bi-Material Media," Engineering Fracture Mechanics, Vol. 28, No. 1, pp.13-20, 1987.

- [10] I.S. Raju, J.H. Crews, Jr., and M.A. Aminpour, "Convergence of Strain Energy Release Rate Components for Edge-Delaminated Composite Laminates," Engineering Fracture Mechanics, Vol. 30, No. 3, pp. 383-396, 1988.
- [11] S.A. Salpekar, I.S. Raju, and T.K. O'Brien "Strain-Energy-Release Rate Analysis of Delamination in a Tapered Laminate Subjected to Tension Load," Journal of Composite Materials, Vol.25 - February 1991.

TABLE 1
MATERIAL PROPERTIES

GLASS/EPOXY

E_{11}	- 50.33 GPa, $(7.3 \times 10^6 \text{ psi})$
E_{22}, E_{33}	- 14.48 GPa, $(2.1 \times 10^6 \text{ psi})$
G_{12}, G_{13}, G_{23}	- 6.07 GPa, $(0.88 \times 10^6 \text{ psi})$
$\nu_{12}, \nu_{13}, \nu_{23}$	- 0.275

GRAPHITE/EPOXY

E_{11}	- 134.45 GPa, $(19.5 \times 10^6 \text{ psi})$
E_{22}, E_{33}	- 11.03 GPa, $(1.6 \times 10^6 \text{ psi})$
G_{12}, G_{13}	- 5.84 GPa, $(0.847 \times 10^6 \text{ psi})$
G_{23}	- 2.98 GPa, $(0.432 \times 10^6 \text{ psi})$
ν_{12}, ν_{13}	- 0.301
ν_{23}	- 0.49

FIGURE CAPTIONS

- Fig. 1 : Schematic of staircase damage pattern for an impacted composite plate [3]
- Fig. 2 : Configuration and loading of a laminate containing impact induced matrix cracks.
- Fig. 3 : Details of laminate analyzed.
- Fig. 4 : Two dimensional finite element mesh of laminate.
- Fig. 5 : Interlaminar normal stress with a 45° matrix crack.
- Fig. 6 : Interlaminar shear stress with a 45° matrix crack.
- Fig. 7 : Variation of G due to delamination at point A ($d=0$).
- Fig. 8 : Variation of G due to delamination at point A ($d=2h$).
- Fig. 9 : Variation of G due to delamination at point C ($b=0$).
- Fig. 10 : Variation of G due to delamination at point C ($b=2h$).
- Fig. 11 : Variation of total G due to delamination growth on either side of the matrix crack.
- Fig. 12 : Variation of G_I due to delamination growth on either side of the matrix crack.
- Fig. 13 : Variation of G_{II} due to delamination growth on either side of the matrix crack.
- Fig. 14 : Variation of G due to delamination growth on either side of the matrix crack (graphite/epoxy).

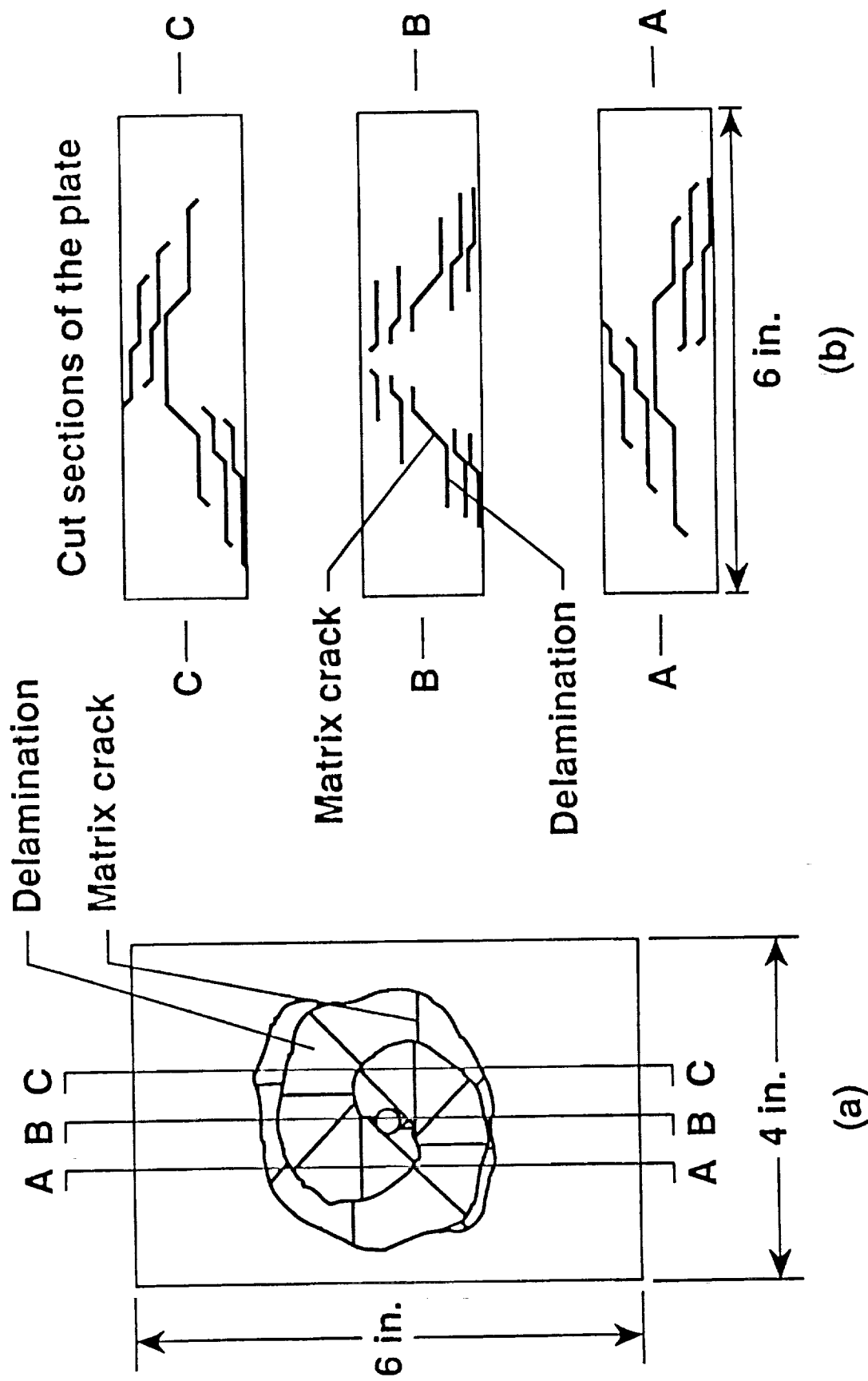


Fig. 1 : Schematic of staircase damage pattern for an impacted composite plate [3]

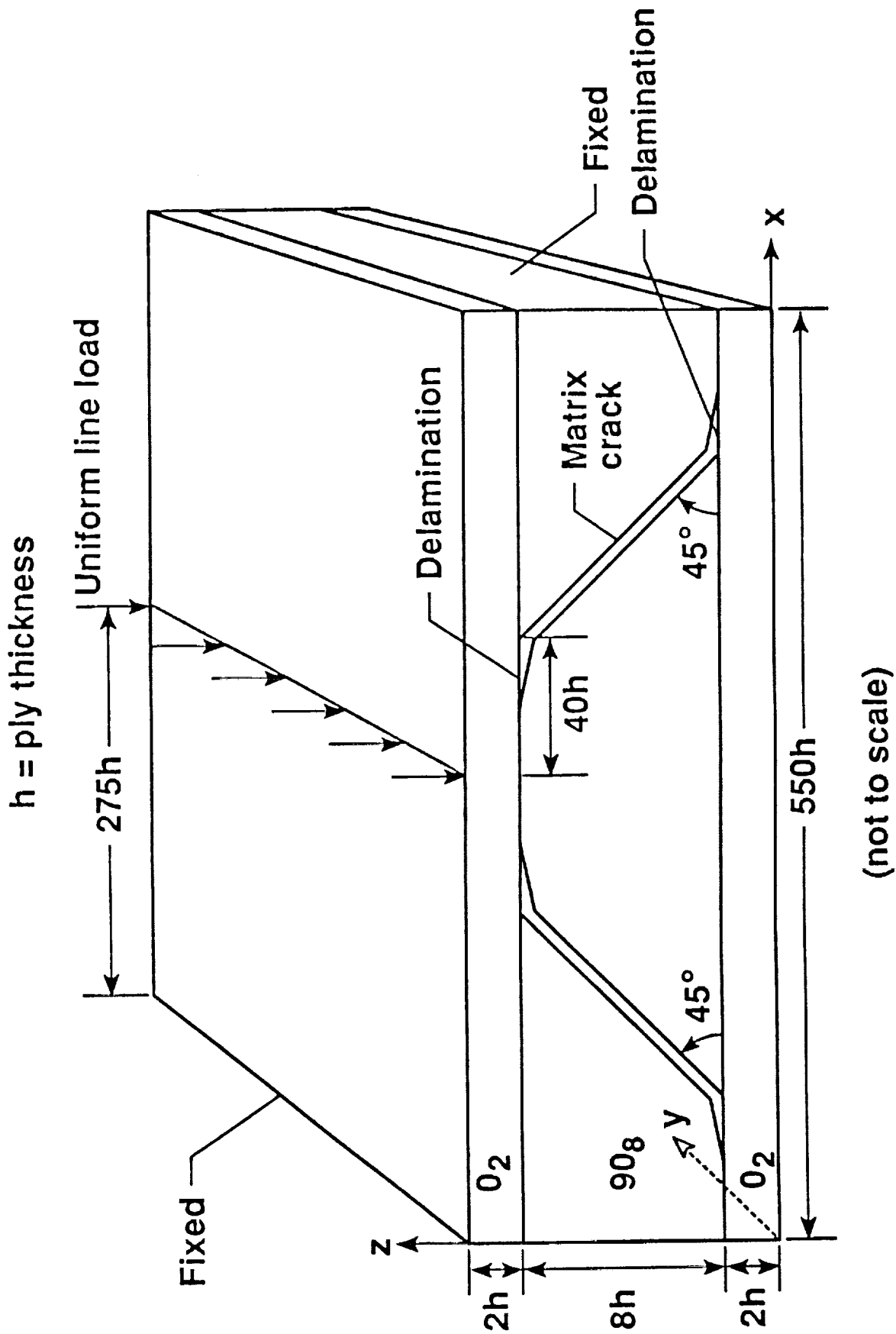


Fig. 2 : Configuration and loading of a laminate containing impact induced matrix cracks.

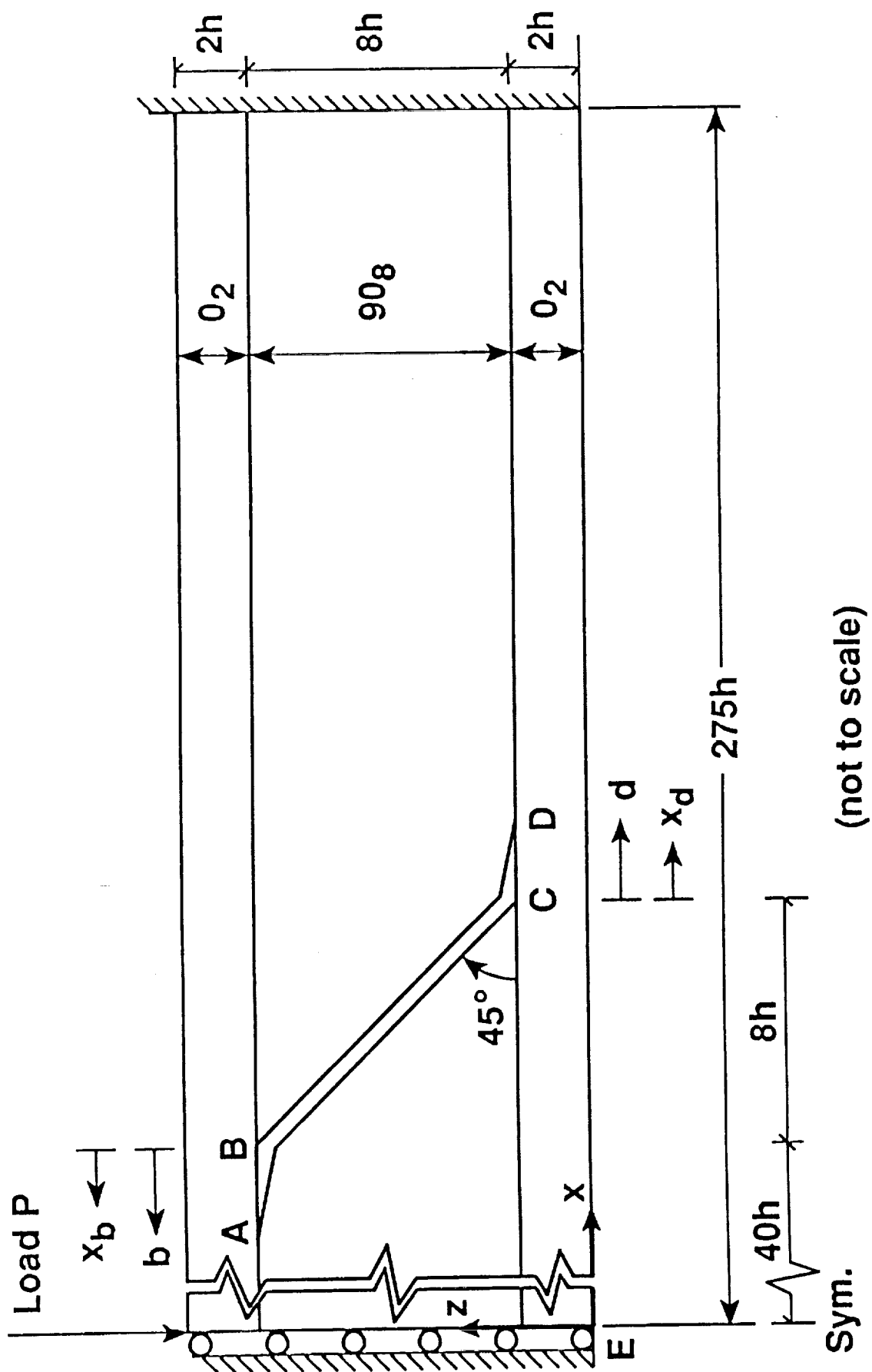


Fig. 3 : Details of laminate analyzed.

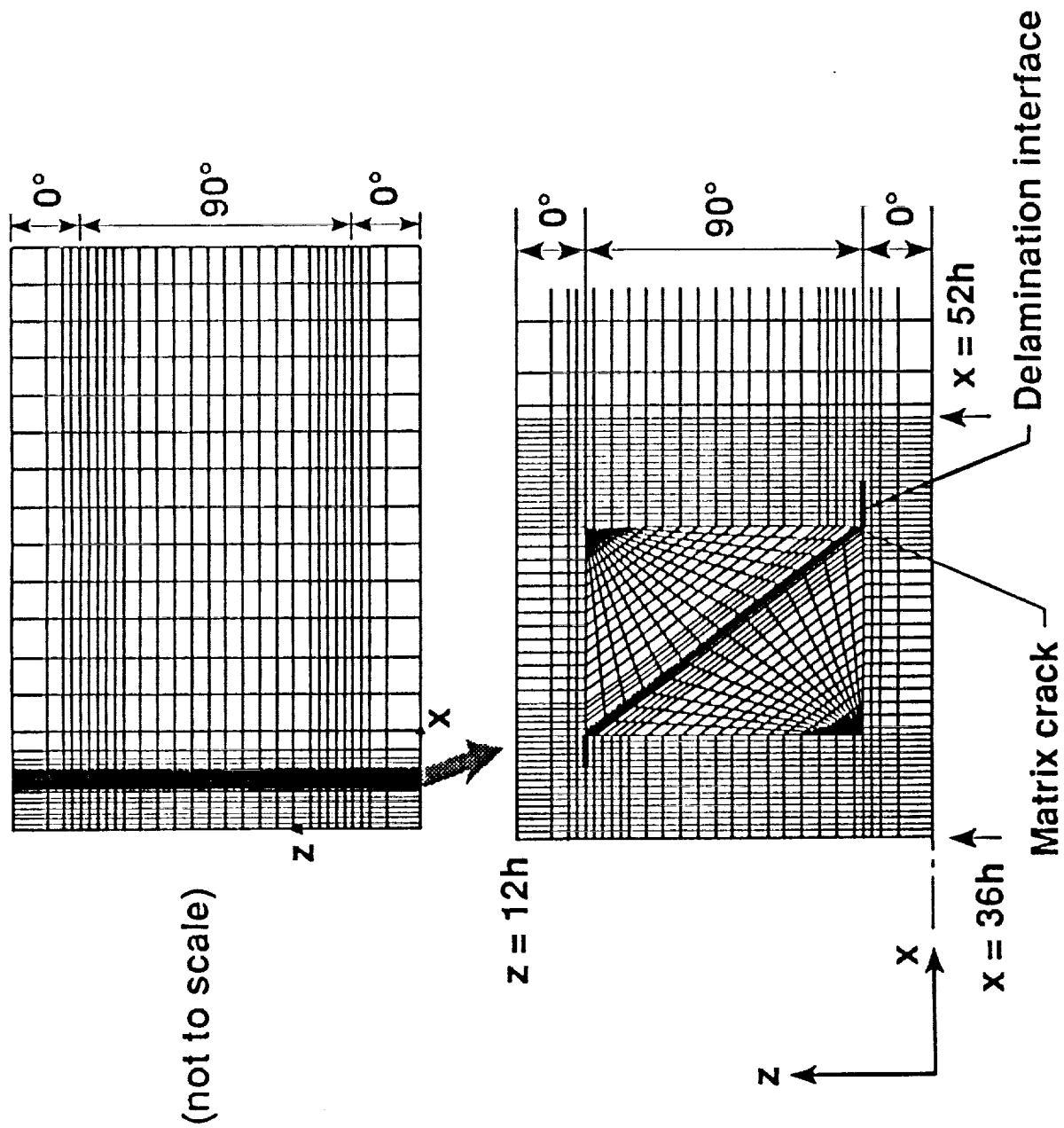


Fig. 4 : Two dimensional finite element mesh of laminate.

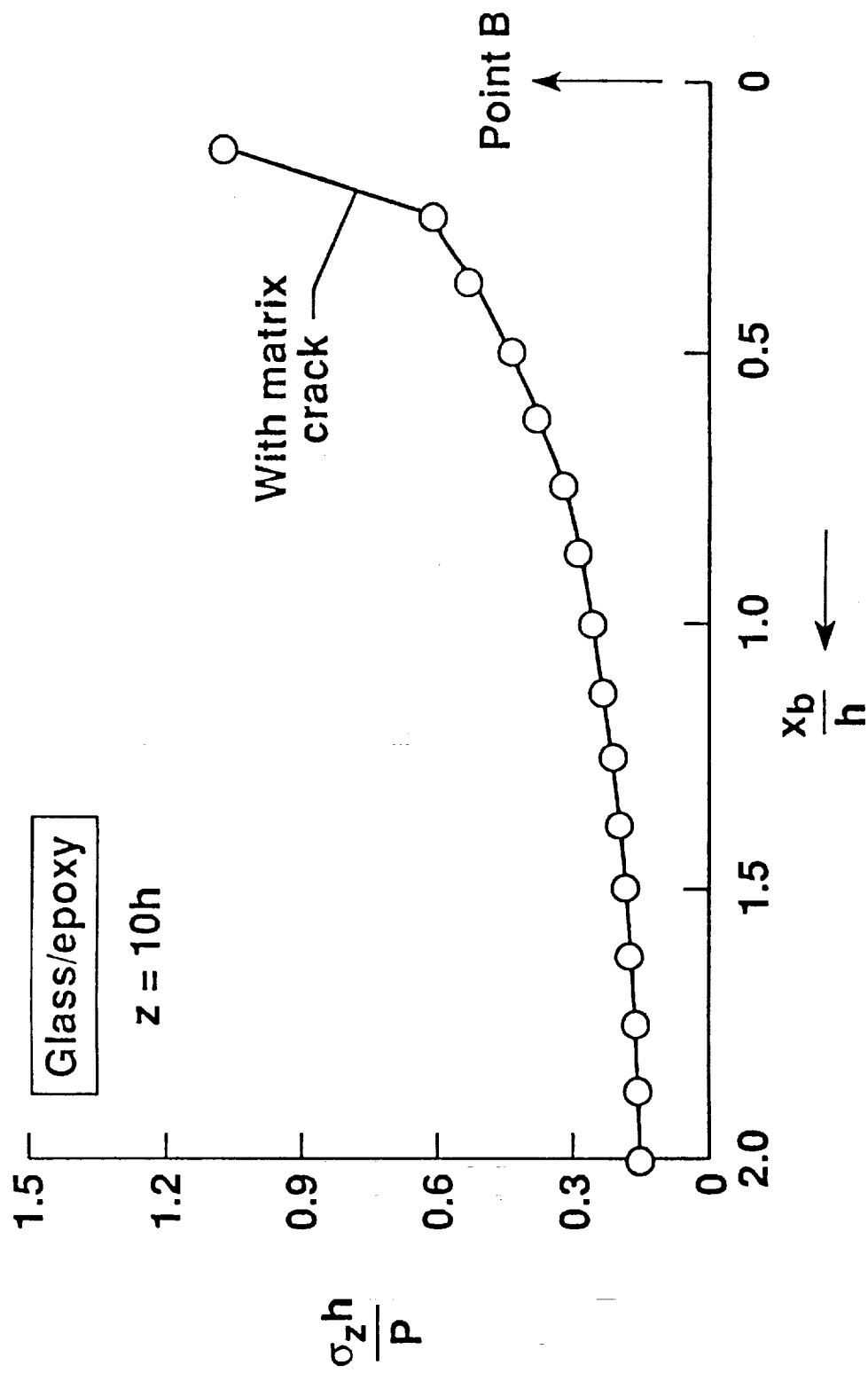


Fig. 5 : Interlaminar normal stress with a 45° matrix crack.

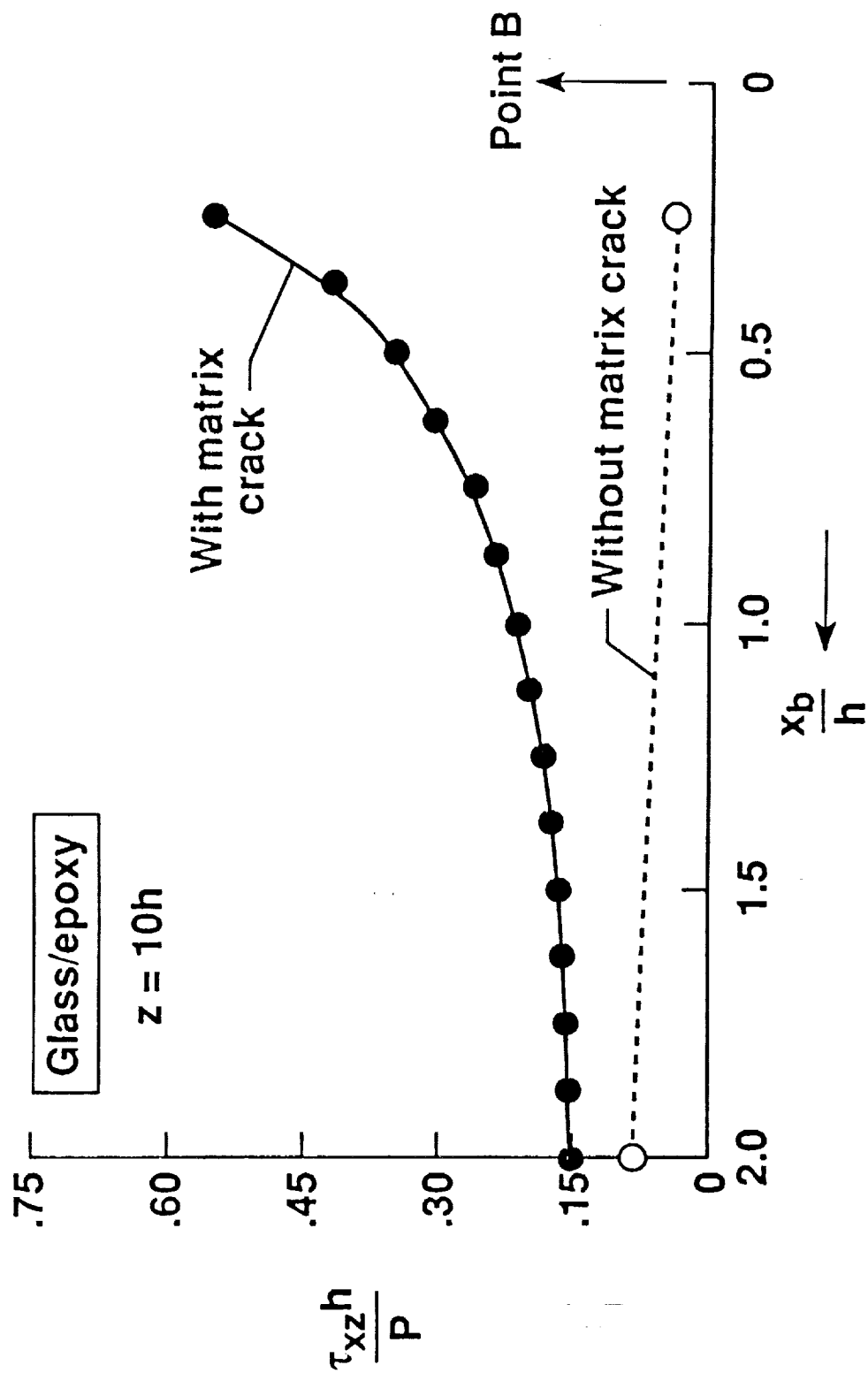


Fig. 6 : Interlaminar shear stress with a 45° matrix crack.

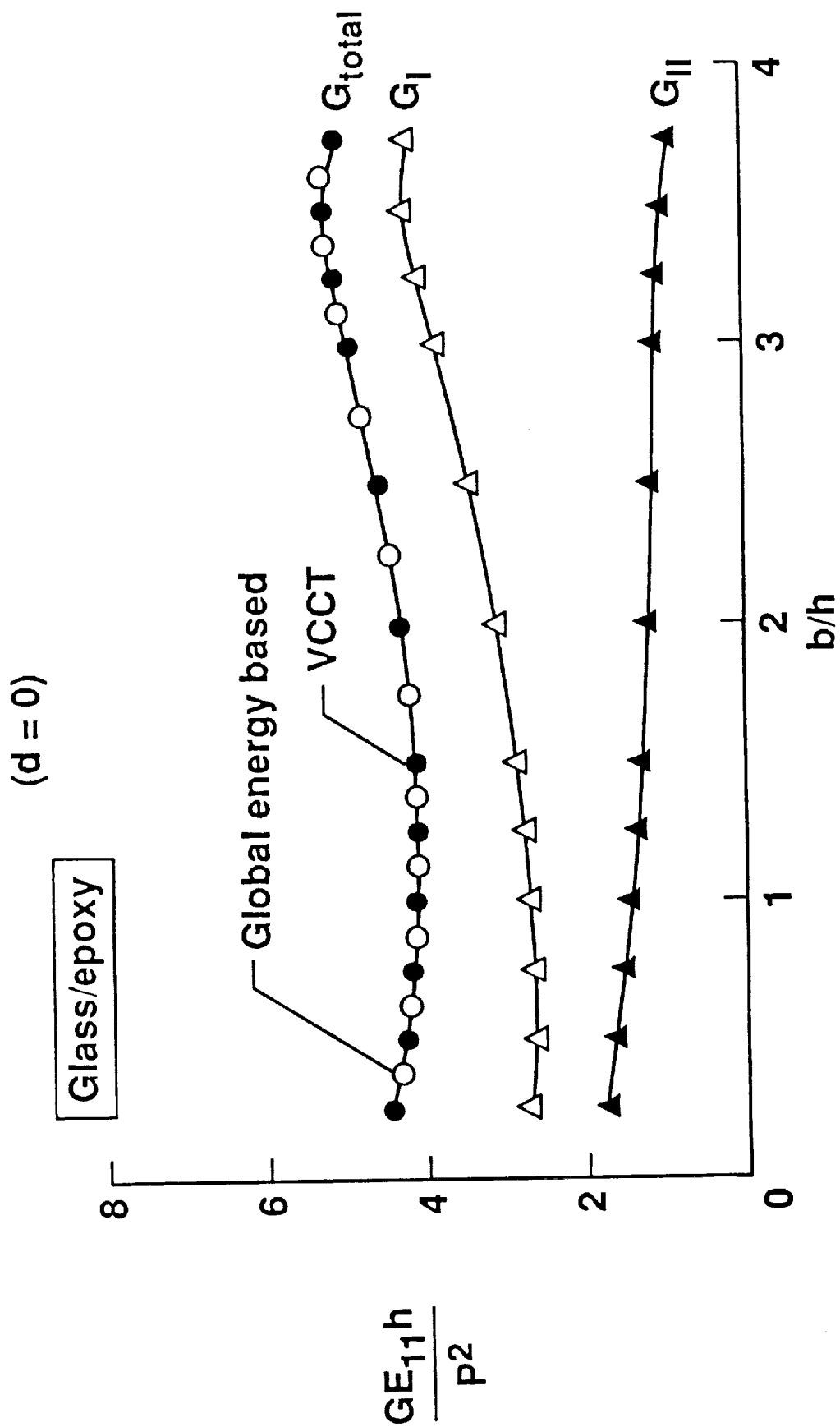


Fig. 7 : Variation of G due to delamination at point A (d=0).

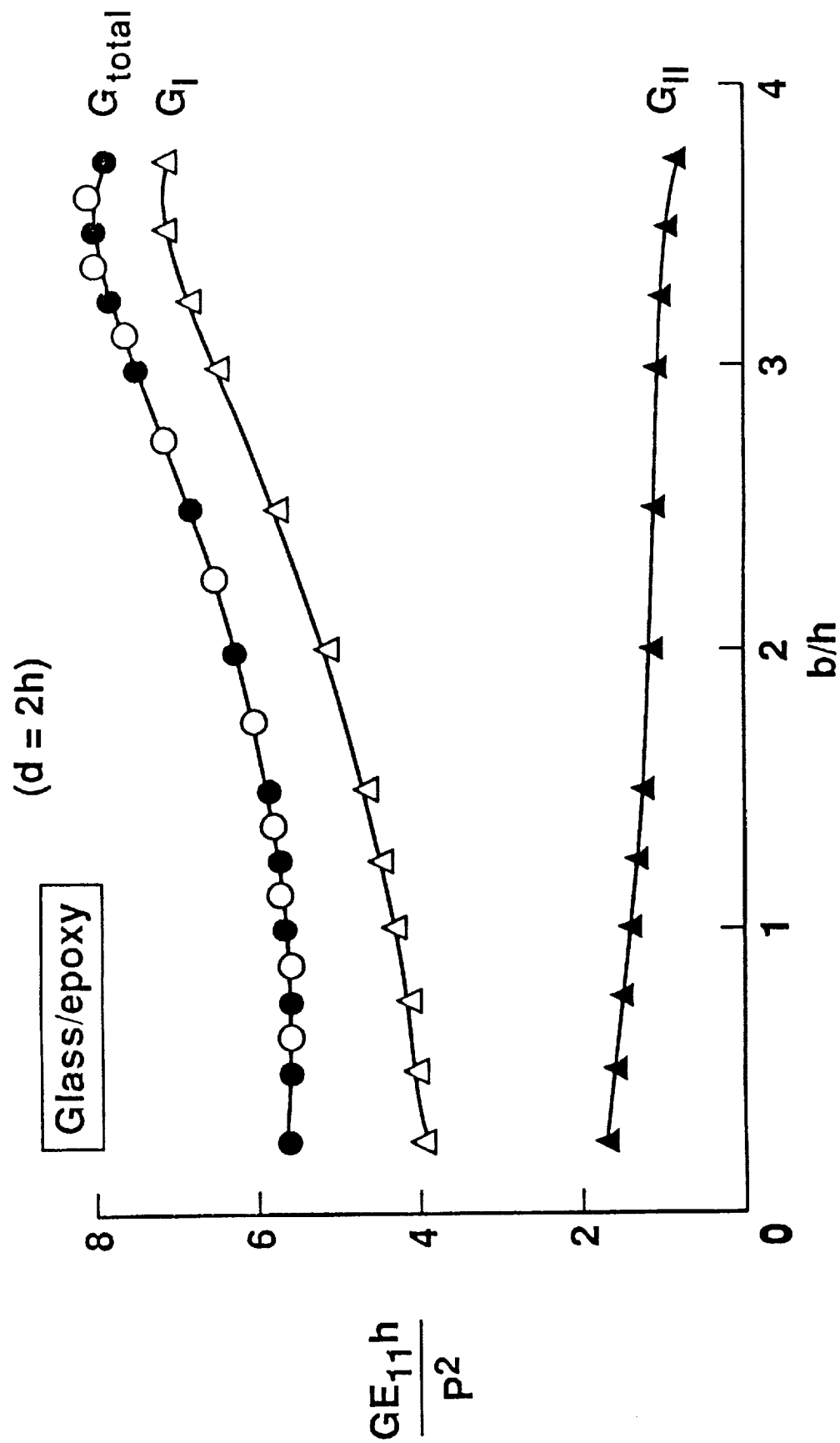


Fig. 8 : Variation of G due to delamination at point A (d=2h).

(b = 0)

Glass/epoxy

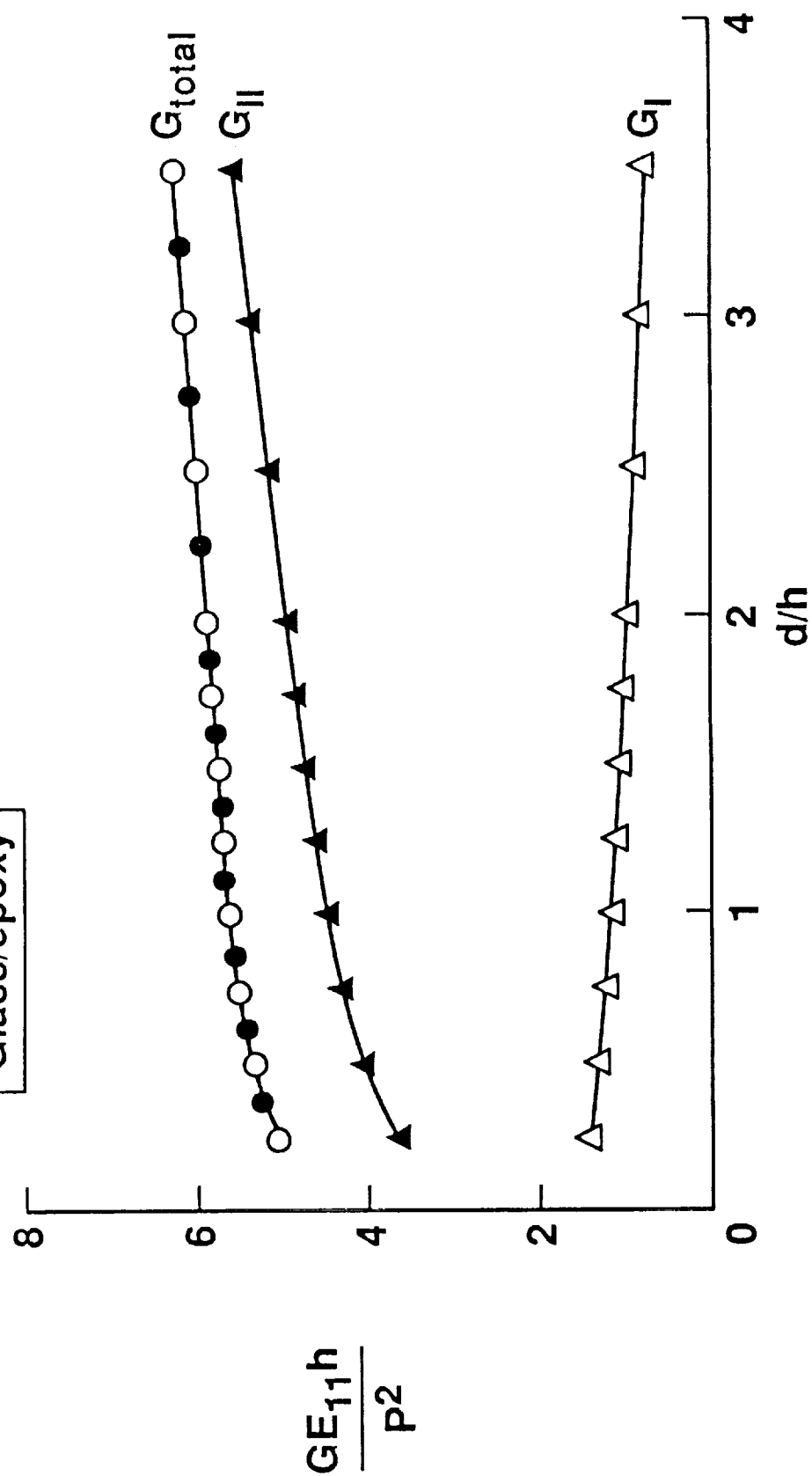


Fig. 9 : Variation of G due to delamination at point C (b=0).

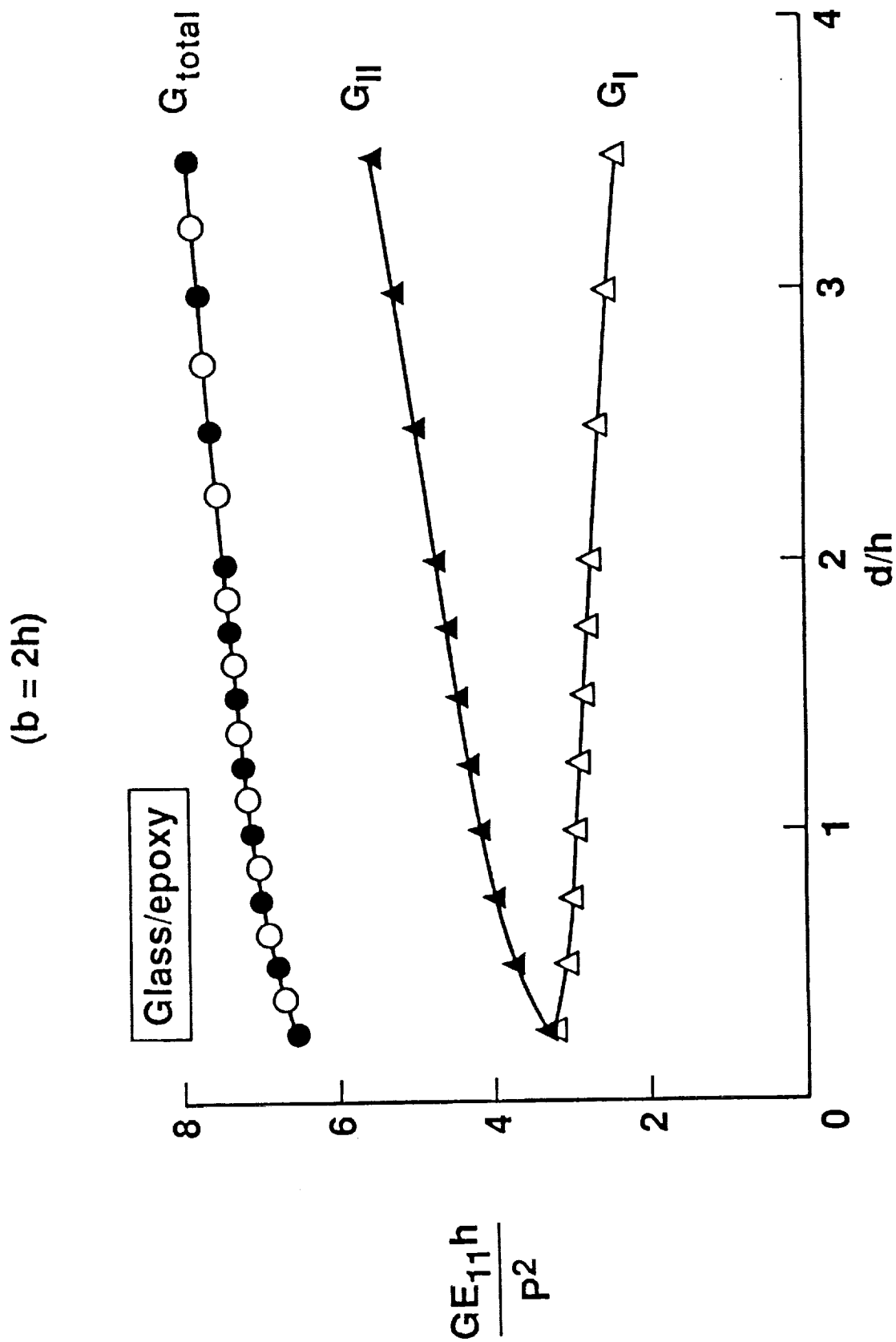


Fig. 10 : Variation of G due to delamination at point C ($b=2h$).

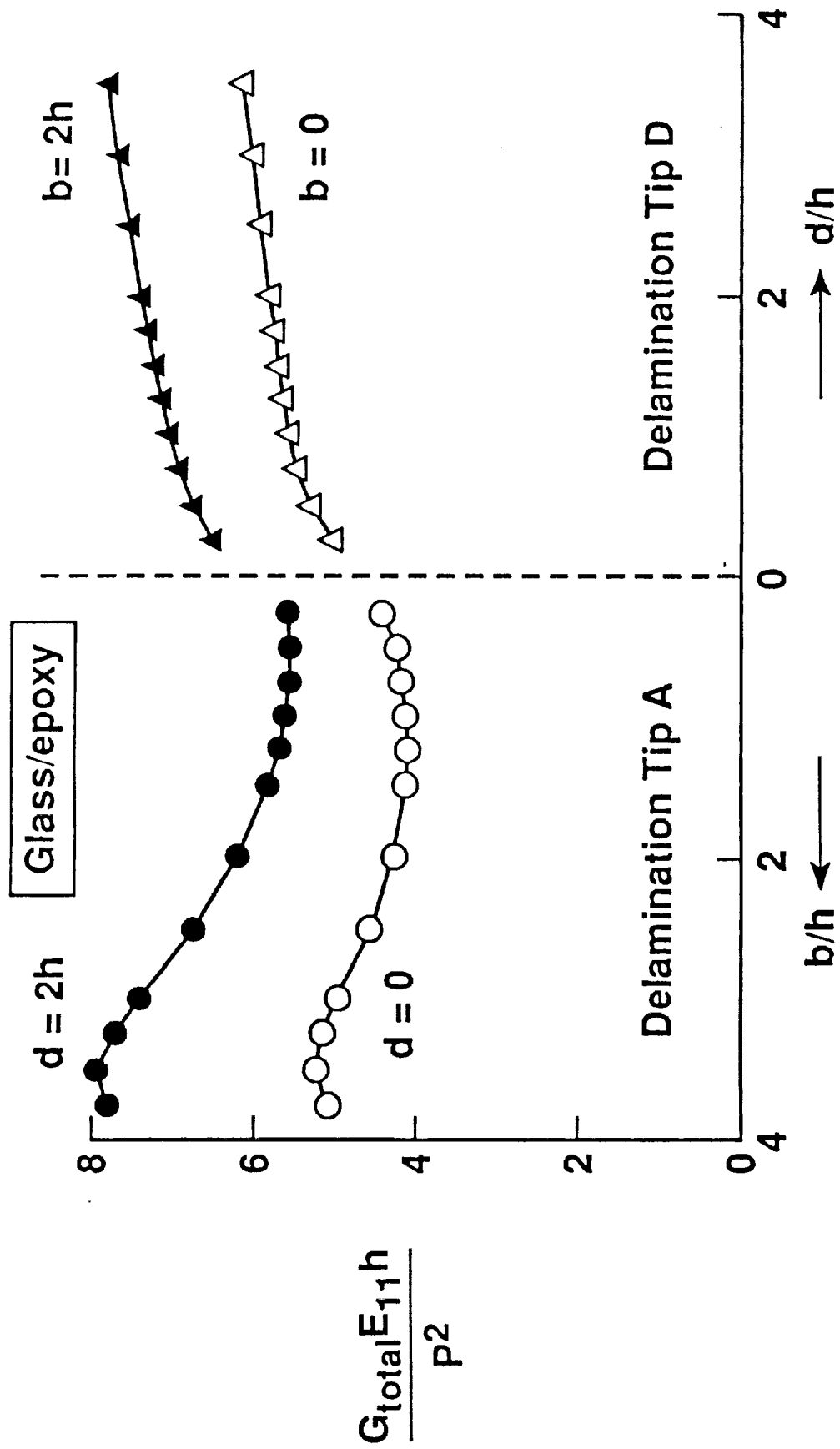


Fig. 11 : Variation of total G due to delamination growth on either side of the matrix crack.

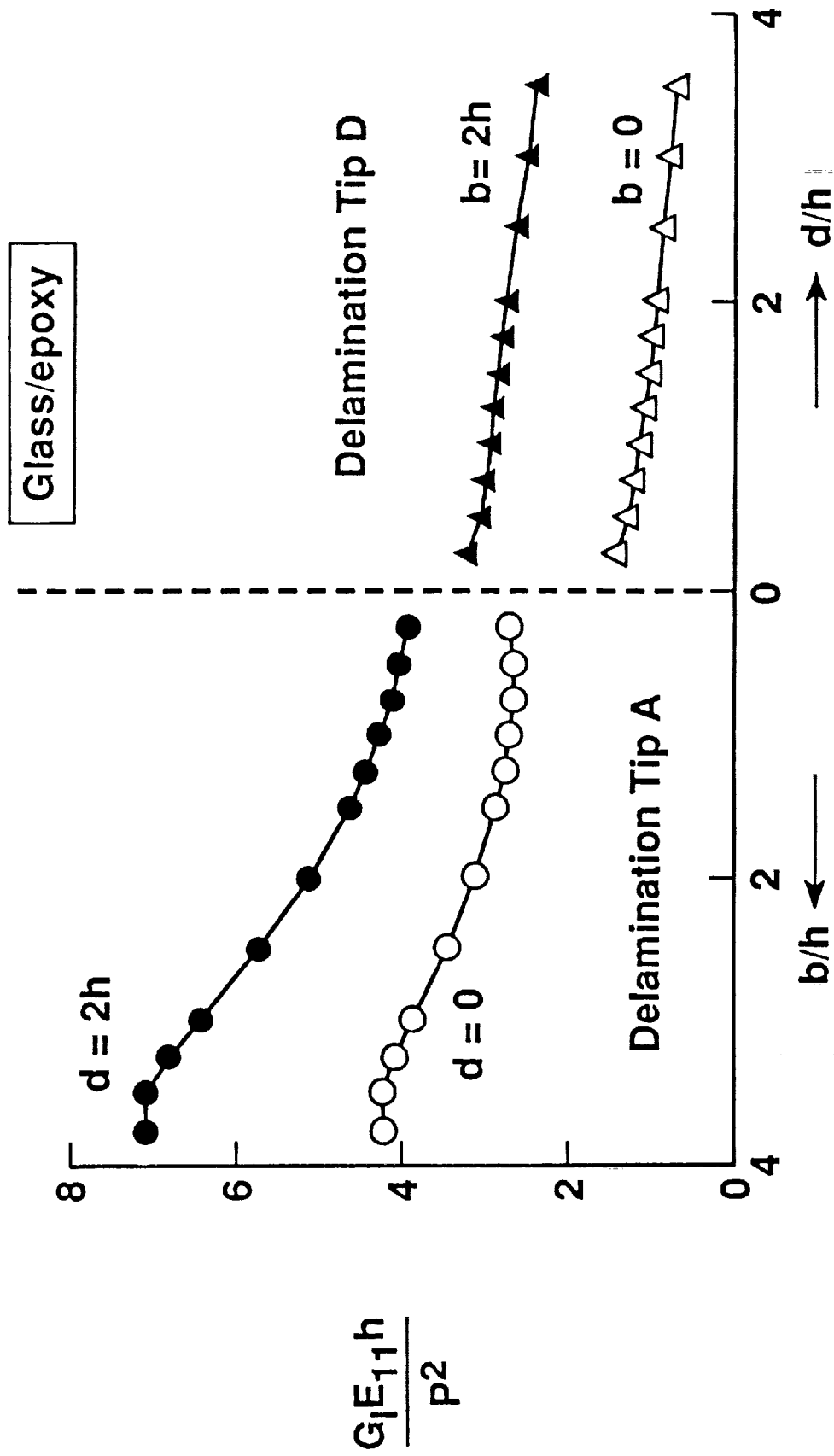


Fig. 12 : Variation of G_I due to delamination growth on either side of the matrix crack.

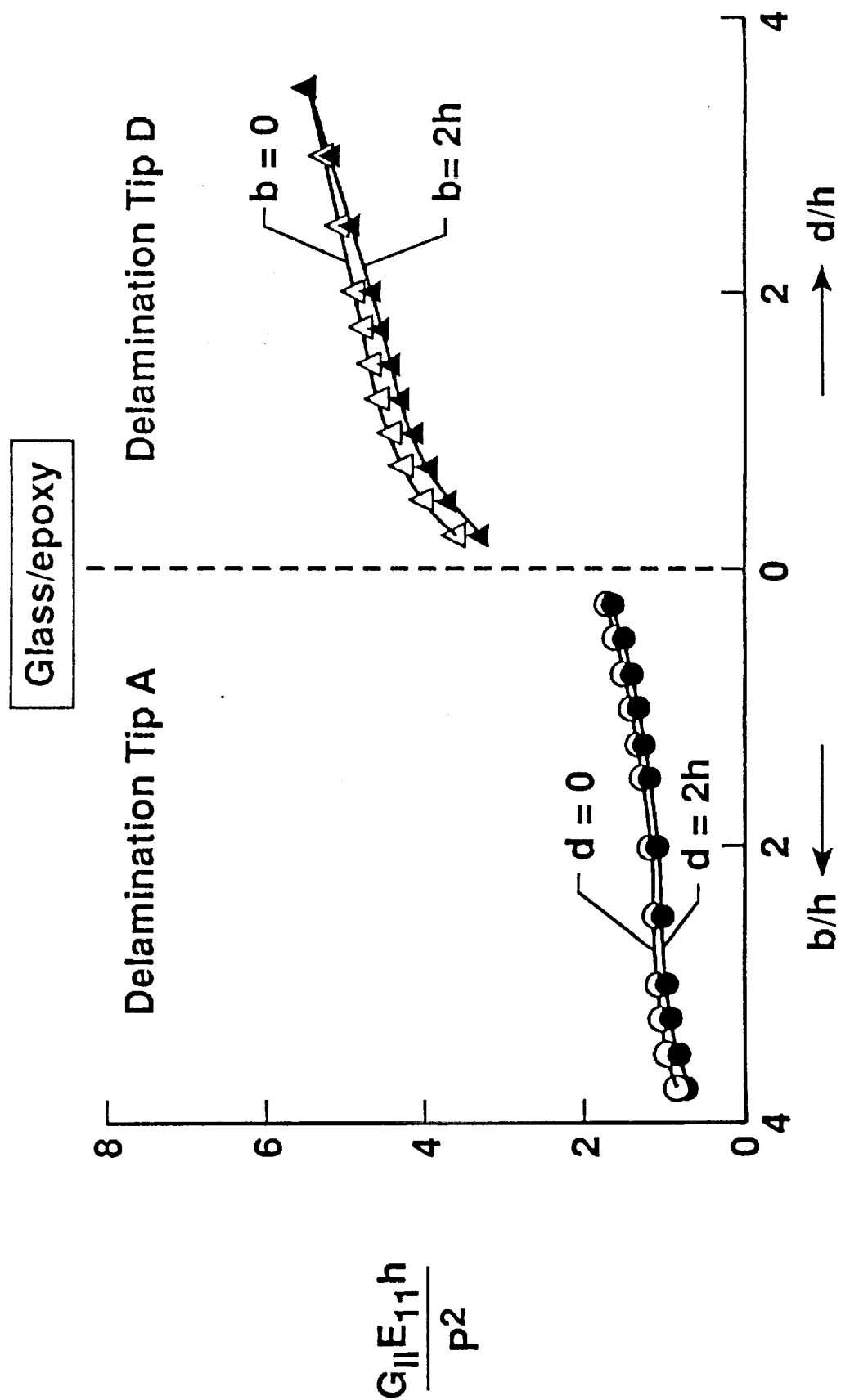


Fig. 13 : Variation of G_{II} due to delamination growth on either side of the matrix crack.

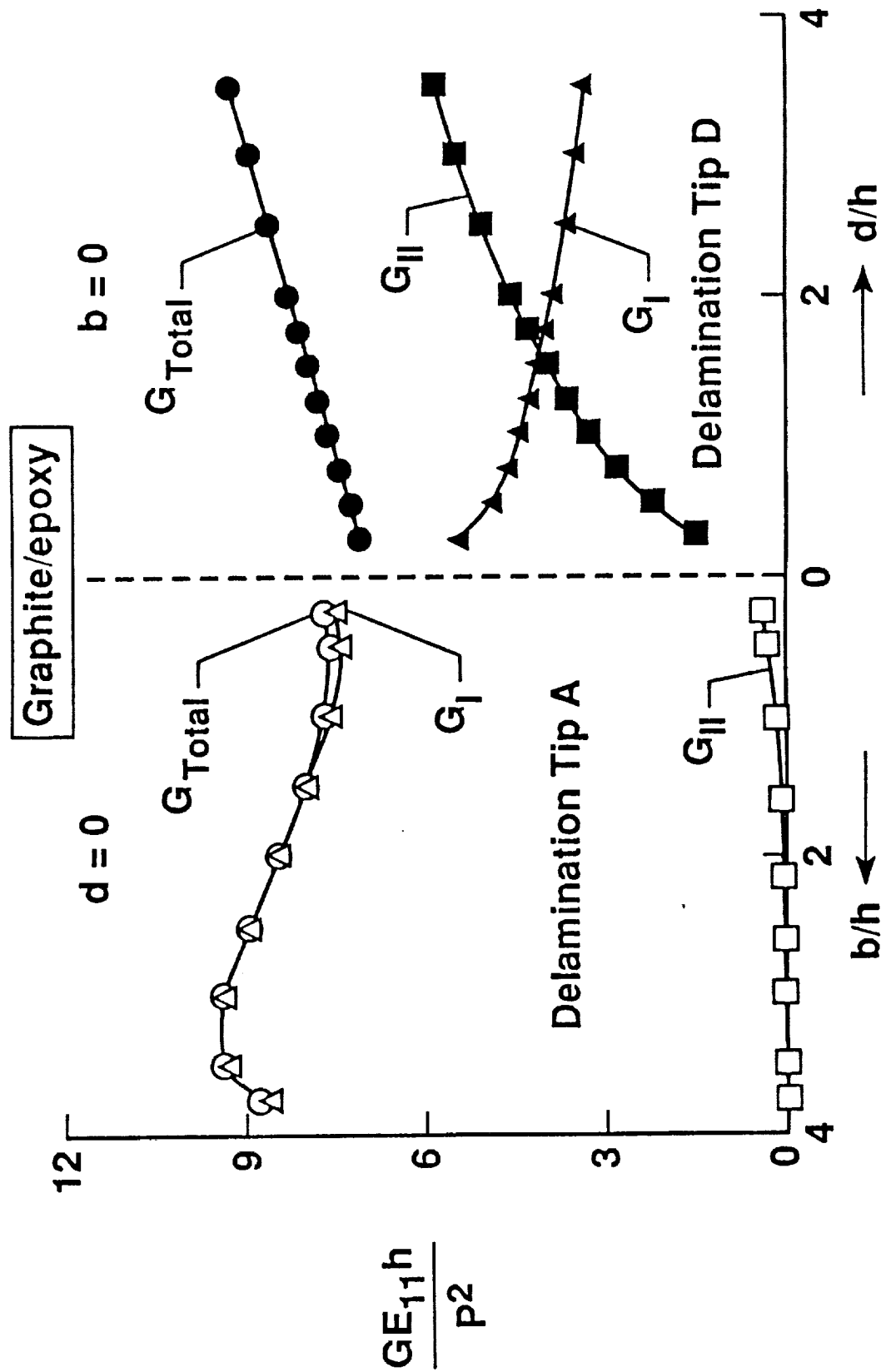


Fig. 14 : Variation of G due to delamination growth on either side of the matrix crack (graphite/epoxy).

REPORT DOCUMENTATION PAGE

Form Approved
OMB No. 0704-0188

Public reporting burden for this collection of information is estimated to average 1 hour per response, including the time for reviewing instructions, searching existing data sources, gathering and maintaining the data needed, and completing and reviewing the collection of information. Send comments regarding this burden estimate or any other aspect of this collection of information, including suggestions for reducing this burden, to Washington Headquarters Services, Directorate for Information Operations and Reports, 1215 Jefferson Davis Highway, Suite 1204, Arlington, VA 22202-4302, and to the Office of Management and Budget, Paperwork Reduction Project (0704-0188), Washington, DC 20503.

1. AGENCY USE ONLY (Leave blank)		2. REPORT DATE November 1991		3. REPORT TYPE AND DATES COVERED Contractor Report	
4. TITLE AND SUBTITLE Analysis of Delamination in Cross Ply Laminates Initiating From Impact Induced Matrix Cracking				5. FUNDING NUMBERS C NAS1-19399 WU 505-63-50-04	
6. AUTHOR(S) S. A. Salpekar					
7. PERFORMING ORGANIZATION NAME(S) AND ADDRESS(ES) Analytical Services and Materials, Inc. 107 Research Drive Hampton, VA 23666				8. PERFORMING ORGANIZATION REPORT NUMBER	
9. SPONSORING / MONITORING AGENCY NAME(S) AND ADDRESS(ES) National Aeronautics and Space Administration Langley Research Center Hampton, VA 23665-5225				10. SPONSORING / MONITORING AGENCY REPORT NUMBER NASA CR-187594	
11. SUPPLEMENTARY NOTES Langley Technical Monitor: Charles E. Harris					
12a. DISTRIBUTION / AVAILABILITY STATEMENT Unclassified - Unlimited Subject Category - 39				12b. DISTRIBUTION CODE	
13. ABSTRACT (Maximum 200 words) Several two dimensional finite element analyses of (0/2/90/0/2) glass/epoxy and graphite/epoxy composite laminates were performed to investigate some of the characteristics of damage development due to an impact load. A cross-section through the thickness of the laminate with fixed ends, and carrying a transverse load in the center was analyzed. Inclined matrix cracks such as those produced by low velocity impact were modeled in the 90 degree ply group. The introduction of the matrix cracks caused large interlaminar tension and shear stresses in the vicinity of both crack tips in the 0/90 and 90/0 interfaces. The large interlaminar stresses at the ends of the matrix cracks indicate that matrix cracking may give rise to delamination. The ratio of mode I to total strain energy release rate, G_I/G_{Total} , at the beginning of delamination, calculated at the two (top and bottom) matrix crack tips was 60 percent and 28 percent, respectively, in the glass/epoxy laminate. The corresponding ratio was 97 percent and 77 percent in the graphite/epoxy laminate. Thus, a significant mode I component of strain energy release rate may be present at the delamination initiation due to an impact load. The value of strain energy release rate at either crack tip increased due to an increase in the delamination length at the other crack tip and may give rise to an unstable delamination growth under constant load.					
14. SUBJECT TERMS Delamination; Impact; Matrix crack; Strain energy release rate; Finite element analysis; Cross ply laminate				15. NUMBER OF PAGES 31	
				16. PRICE CODE A03	
17. SECURITY CLASSIFICATION OF REPORT Unclassified	18. SECURITY CLASSIFICATION OF THIS PAGE Unclassified	19. SECURITY CLASSIFICATION OF ABSTRACT	20. LIMITATION OF ABSTRACT		